SALT DAMAGE IN WOOD: CONTROLLED LABORATORY EXPOSURES AND MECHANICAL PROPERTY MEASUREMENTS[1]

Grant T. Kirker

Research Forest Products Technologist
Wood Durability and Protection
USDA Forest Service, Forest Products Laboratory
Madison, WI
E-mail: grant.kirker@usda.gov

Christian Brischke

Researcher and Lecturer
University of Goettingen
Wood Biology and Wood Products
Göttingen, Germany
E-mail: christian.brischke@uni-goettingen.de

Leandro Passarini†

Manager-Scientist
Agriculture-Bioprocédés-Breuvages-Environnement
Collège communautaire du Nouveau-Brunswick (CCNB-INNOV)
Grand-Sault, NB, Canada
E-mail: leandro.passarini@ccnbca

*Samuel L. Zelinka**†

Project Leader
Building and Fire Sciences
USDA Forest Service, Forest Products Laboratory
Madison, WI
E-mail: samuel.l.zelinka@usda.gov

(Received June 2019)

Abstract. Salt damage in wood can be recognized by its stringy appearance and is frequently observed in wood used in maritime structures and buildings built near the ocean. Whereas salt-damaged wood is common, little is known about the mechanism by which salt water alters the wood structure. There is no information on the effects of salt damage on the mechanical properties of wood. In this study, a laboratory method for creating salt damage in other porous materials was applied to wood. Wood pillars were placed in a reservoir of 5 M NaCl and exposed to a 40% RH environment. Capillary action pulled the salt water to the upper part of the pillars which were dry. Large deposits of effloresced salts were observed. The changes in mechanical properties caused by salt were measured by the high-energy multiple impact (HEMI) test. Salt damage caused a reduction in the resistance to impact milling (RIM) of 6.5%, and it was concluded that salt damage causes only minor effects on the strength of wood. The tests were not conclusive as to the exact mechanism of salt damage in treated wood. However, diffusion of mineral ions through the cell wall was found to be a key step in the salt damage mechanism.

Keywords: Defibrillation, salt water, chemical modification, wood damage mechanisms, resistance to impact milling (RIM).

* Corresponding author
† SWST member
[1] This article was written and prepared by US Government employees on official time, and it is therefore in the public domain and not subject to copyright.

Wood and Fiber Science, 52(1), 2020, pp. 44-52
https://doi.org/10.22382/wfs-2020-005

INTRODUCTION

Salt damage is a phenomenon that can negatively impact porous building materials, including wood. The effects of salt damage have been widely documented in mortars, masonry, and other cementitious materials (Price and Brimblecombe 1994; Charola 2000; Flatt 2002; Scherer 2004, Derluyn et al 2014a, 2014b). In these materials, salt damage causes spalling of the outer layers of the material and can be easily identified by white salt residues deposited on the surface of the material (efflorescence). Salt-damaged wood has a "fuzzy" surface from defibrillated tracheids and is sometimes misidentified as fungal decay (Kirker et al 2011).

There has been a significant amount of research examining the mechanisms of salt damage in nonbiological porous materials. In these materials, the salt damage is caused by a mechanical interaction from salt crystallization in the pores (Scherer 2004). The study of the behavior of fluids in porous media (poromechanics) can be used to describe the conditions under which salt damage will occur. In brief, water with dissolved salt is absorbed by the material and held within the material pores. As the material dries, the salt concentration increases until it reaches saturation. In large pores, crystals can nucleate and grow within the pore without causing damage (Flatt 2002). However, in small pores, the solution becomes supersaturated. Eventually, there is a point at which the energy required to form a crystal and expand the pore is less than the energy to further saturate the solution. At this point, crystals will nucleate in small pores beneath the surface (subflorescence) which causes internal stresses and eventually spalling. Although this mechanism is accepted for porous materials in general, it has not been universally accepted in wood.

Salt damage in wood has received only minor attention in the literature (Parameswaran 1981; Johnson et al 1992; Jones et al 2011; Kirker et al 2011; Ortiz et al 2014). Most salt-damaged wood occurs in marine pilings above the waterline. However, salt-damaged wood has also been observed in attic spaces near the coast, wooden decks on which deicing salts were used, and in wooden ships where salt was used to pack the hold. In all cases, the salt-damaged wood is easy to identify (Fig 1). Macroscopically, the wood has a rough, stringy appearance (Fig 1[a]). Microscopically (Fig 1[b]), the tracheids are separated and salt crystals can be found with a scanning electron microscope.

Several different theories have been proposed to explain salt damage in wood. A mechanical damage mechanism was proposed by Johnson et al (1992) who observed cuboidal sodium chloride crystals in salt-damaged wood. This mechanism is essentially the same as those proposed by Scherer and others for salt damage in masonry materials. By contrast, Parameswaran (1981) and, later, Ortiz et al (2014) proposed that salt damage is a result of chemical changes to the cell wall. This mechanism was based on observations of a wood storage facility used to house potash. Potash was characterized as potassium chloride with a pH of 6.94. Parameswaran noted

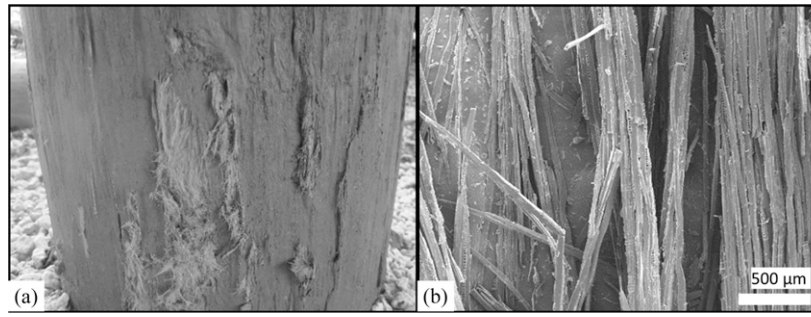

Figure 1. Examples of salt-damaged wood at macroscale (a) and microscale (b).

that fewer sugars and lignin were found in the salt-damaged wood. The degradation of these wood components is similar to what is observed in alkaline pulping of cellulosic materials and decay caused by white-rot fungi. Because of this, Parameswaran attributed the damage in the wood to alkaline pulping, where the alkaline environment came from the potash.

It is interesting to note that in wood, salt damage preferentially damages the middle lamella rather than the secondary cell wall. Physically, it could be that the pore structure and connectivity of the middle lamella is better suited for the nucleation and growth of salt crystals. Chemically, calcium plays an important role in the structure of the middle lamella, serving as a crosslinking agent for pectin, hemicelluloses, and lignin (Terashima et al 1993). When other salts infiltrate the middle lamella, it is possible that the positively charged cations could disrupt these bonds or displace the calcium ions. Further work is needed to understand if salt damage in wood is a purely physical damage mechanism (as it is in other porous materials) or if there are chemical breakdown mechanisms as well.

Previous research on salt damage in wood has only examined the physical changes that occur during salt damage, and no mechanical properties of salt-damaged wood are available. Although salt damage in wood was traditionally believed to be a cosmetic (nonstructural) concern, recently, a structural failure of salt-damaged wood has been observed on the ship *Eureka* located at the San Francisco Maritime National Historical Park (Kirker et al 2016; Zelinka and Kirker 2018). The bilge of the *Eureka* was packed with salt to prevent fungal decay; one of the joists in the bilge exhibited a crushing failure where it met a support (Fig 2). Although anecdotal, this observation of a structural failure highlights the importance of understanding the effects of salt damage on the mechanical properties so that the correct strength values for salt-damaged wood can be assigned in condition assessments.

Here, we present a controlled laboratory experimental methodology for examining salt damage in wood by modifying the method of Scherer (Scherer 2004). We illustrate how this method can be used to examine the salt damage under repeatable conditions and present results on how salt damage affects the strength by examining its resistance to impact milling (RIM). We then discuss how this method can be used to refine models of salt damage in wood and highlight further research needs.

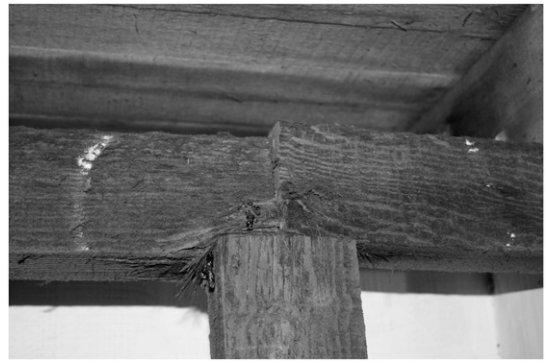

Figure 2. Crushing failure on a salt-damaged joist in the bilge of the *Eureka*.

METHODS AND MATERIALS

Materials

Southern pine (*Pinus* spp.) sapwood was examined in this study. The specimens were 25 25 300 mm (longitudinal). The grain orientation varied between samples, and in no case was the sample cut with true radial or tangential faces; in most cases, the grain angle was approximately 45° to the sample faces. Before exposure, the samples were conditioned in a laboratory at 50% RH and an approximate starting MC of 9% (Glass and Zelinka 2010).

Exposure method. The salt damage was affected through the method of Scherer with modifications shown in Fig 3 (Scherer 2004). The wood was partially submerged in a 5 M NaCl solution. Although much higher than the salinity of seawater, this concentration was used to match previous research on salt-damaged materials which examine nearly saturated solutions as the concentration near the material surface is often

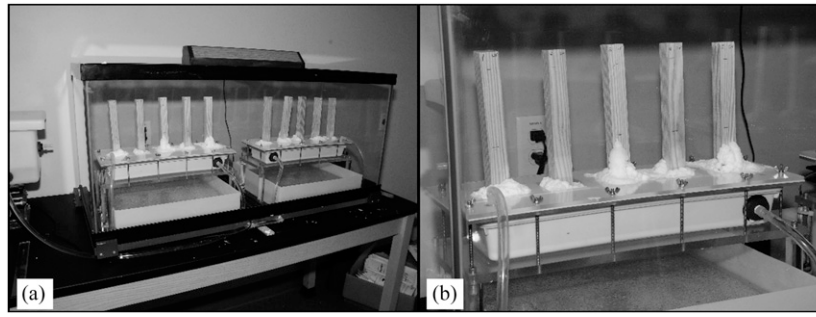

Figure 3. Photographs of the experimental methods used to control the salt exposure. (a) The apparatus including the enclosure to maintain the RH; (b) a close-up view of the wood samples in the salt solution.

close to saturation (Lewin 1982; Scherer 2004). Slightly above the waterline, the wood was sealed to the trough containing the solution with gasketing. By sealing the solution, it was possible to control the RH above the waterline. The RH was controlled by placing the entire apparatus inside of an aquarium with a large saturated salt solution of $CaCl_2$ to fix the RH at 40% (Greenspan 1977); the experiments were performed at room temperature 21°C 5°C. Time-lapse photographs were taken throughout the experiment to monitor the progression of the salt damage. To see how salt damage progressed with time, two different durations of experiments were run: 4 and 12 wk ($n = 10$ for each condition).

Physical changes. The sample mass was taken 1) before the exposure, 2) on removal from the test apparatus, 3) after the effloresced salt was removed, 4) after oven drying postexposure, and 5) after reconditioning in the same temperature and humidity conditions to which the original sample was conditioned. In addition to these measurements, the height of the absorbed water was also measured. Two replicates were cut length-wise through the middle and photographed. The coloration of the wood was used as an indication of the height of the absorbed water.

Mechanical changes. The changes in the mechanical properties were examined using the high-energy multiple-impact (HEMI) method developed by Brischke et al (2006) and Rapp et al (2006). The HEMI method was developed for measuring changes in structural integrity on samples affected by fungal decay. The HEMI test uses very little material, and the results are independent of the orientation and density of growth rings within the sample (Rapp et al 2006). Because of these advantages, the HEMI method was selected so that the structural integrity of the salt-damaged specimens could be examined as a function of their proximity to the waterline.

The HEMI method was performed by grinding 10 rectangular prisms, each of which had dimensions 5 10 17 mm. Four replicates were tested for each experimental combination so that there were 40 (ie 4 10) prism for each condition. Prisms were cut from three distinct 75-mm regions along the vertical position of the salt-exposed samples: "bottom," "middle," and "top." These 75-mm regions were cut along the grain in 10-mm segments, resulting in 25 25 10 mm segments. These segments were then sliced in 5-mm increments along a 25-mm face, resulting after accounting for the saw kerf in four 5-mm-thick prisms: two of which were fully exposed to the environment and two of which were from the center of the sample. These two groups were kept separated and examined as separate groups to see if the structural integrity was different on the exposed surfaces as opposed to the inside of the sample. Finally, the remaining 25-mm side was reduced to 17 mm to create prisms that were 5 10 17 mm. The HEMI method was performed on prisms that had 0, 4, and 12 wk of exposure to the salt chamber.

To measure the RIM, 10 prisms (1 replicate) were placed in the bowl (140 mm in diameter) of a heavy vibratory impact ball mill (Herzog HSM 100-H; Herzog Maschinenfabrik, Osnabrück, Germany), together with one steel ball of 35 mm diameter for crushing the specimens. Three balls of 12 mm diameter and three of 6 mm diameter were added to avoid small fragments from being trapped in the corner and ensure impact with smaller wood fragments. The bowl was shaken for 60 s at a rotary frequency of 23.3 s^{-1} and a stroke of 12 mm. The fragments of the 10 prisms were fractionated on a slit sieve according to ISO 5223 with a slit width of 1 mm using an orbital shaker at an amplitude of 25 mm and a rotary frequency of 200 min^{-1} for 2 min (Anon 1992). The following values were calculated:

$$I = \frac{m_{10}}{m_{\text{all}}} \quad 100 \,[\%, \tag{1}$$

where I is the degree of integrity (%); m_{10} is the oven-dry mass (g) of the 10 biggest fragments; and m_{all} is the oven-dry mass of all fragments (g).

$$F = \frac{m_{\text{fragments} < 1\text{mm}}}{m_{\text{all}}} \quad 100 \,[\%, \tag{2}$$

where F is the fine percentage; $m_{\text{fragments}<1\text{mm}}$ is the oven-dry mass of fragments smaller than 1 mm (g); and m_{all} is the oven-dry mass of all fragments (g).

$$\text{RIM} = \frac{(I \quad 3 \quad F) + 300}{400} \,[\%, \tag{3}$$

where RIM is the resistance to impact milling (%); I is the degree of integrity (%); and F is the fine percentage (%).

RESULTS AND DISCUSSION

Figure 4 is a time-lapse composite image of the samples exposed for 12 wk. Efflorescence appears directly above the gasket, and this amount of effloresced salt increases with time. Once the crystals formed on top of the gasket, the crystals were able to draw NaCl from the reservoir below through capillary action along the surface of the wood. This "short-circuiting" happened in all cases, although several different sealing techniques were used. No changes were visible at the top of the wood specimen. In some cases, cracks can be observed in the wood. The largest cracks occurred slightly above the large salt deposits.

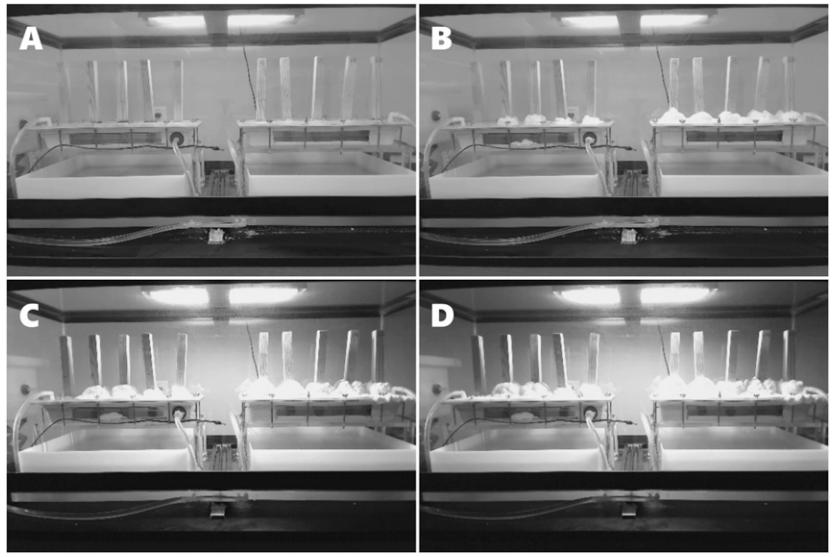

Figure 4. Time-lapse photographs of the 12-wk test. Clockwise from top left: 0, 4, 8, and 12 wk of exposure.

The height of the water rise within the samples can be observed in Fig 5, which is a photograph of longitudinal cross sections of the samples taken immediately after removal from the 4-wk salt exposure. Two cross sections are shown: one sample was cut along a primarily tangential plane and the other was cut along a radial plane. The height of the water rise can be observed by the dark coloration in the wood, and the highest level of the water rise is marked with an arrow in the image. The water rise is highest in the latewood. This is not surprising as it has been shown that liquid water transport is more favorable in the latewood with smaller lumina dimensions than earlywood (Zillig et al 2006; Zillig 2009). The height of the water rise on the measured samples varied between 100 and 125 mm. This height corresponded with the height of the effloresced salt deposits on the outside of the samples.

The sample masses increased in both the 4 and 12-wk tests. To obtain the posttest mass, effloresced salt was mechanically removed and samples were reconditioned in a room at 50% RH after the exposure to minimize any mass differences caused by MC. The average posttest masses of the 4-wk samples was 104 g (10 g, standard error) and 101 g (6 g) for the 12-wk samples compared with the starting masses of 96 (10 g). The percent mass change of each sample was also calculated. The samples exposed for 4 wk had an average mass gain of 8.5% 0.4%, and the samples exposed for 12 wk had an average mass gain of 9.2% 0.4%.

The results of the HEMI method can be seen in Fig 6 which plots the RIM as a function of exposure time. Measurements taken from the inner core were compared with the prisms cut from the exterior of the sample, and the results were compared using a student's *t*-test. Results were found to be insignificant at the 5% level (*t*-values ranged from 0.11 to 0.84). Therefore, these results were combined into a single measurement of the RIM at each spatial position. Not surprisingly, the measurements taken from the bottom of the specimen showed the largest decrease in the structural integrity. In this case, the RIM decreased from 79.8% to 74.5%, or a decrease in properties of 6.5%, and this decrease happened within the first 4 wk of exposure. By contrast, the RIM values measured in the middle of the sample show a degradation in properties throughout the exposure time, decreasing from 79.8% to 77.4% at 4 wk to 75.2% at 12 wk. The measurements taken at the top of the sample show a slight decrease from 79.8% to 78.4% and 78.2% at 4 and 12 wk, respectively.

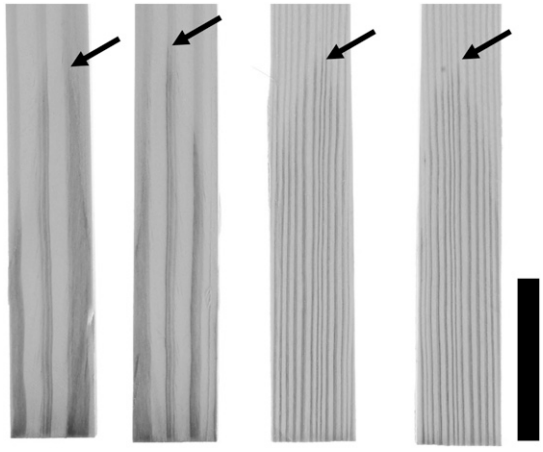

Figure 5. Photograph of cross sections cut immediately after the 4-wk test. The coloration was used to determine the height of the water rise (highlighted with arrows). Scale bar = 50 mm.

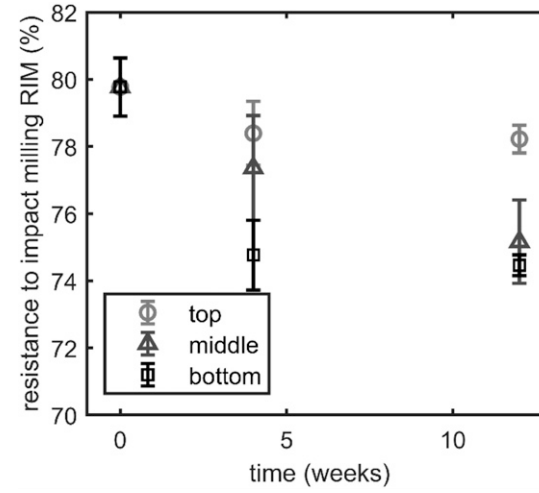

Figure 6. Change in the resistance to impact milling as a function of exposure time in the salt chamber.

From these experiments, it appears that salt damage causes small but measurable permanent changes to the structural integrity of the wood. In service, salt damage can be easily observed by the "stringy" texture of the wood surface. However, to date, it was unclear whether salt damage could cause structural damage to the wood. The data show that salt damage causes a 6.5% reduction in the RIM. To put this reduction into context, a 6% loss in RIM is similar to the effects caused by 15% mass loss by a white-rot fungi or 2% to 4% mass loss by a brown-rot fungi (Brischke et al 2006). A 6% reduction in RIM is also observed for mild heat treatments (3% mass loss) and 90kGy of gamma radiation (Rapp et al 2006; Despot et al 2007).

This reduction in structural integrity did not change between the 4- and 12-wk exposures for the samples immersed in salt water, and it is possible that the salt damage had progressed to its end value at 4 wk. In light of these observations, it appears safe to conclude that salt damage causes a less than 10% decrease in structural integrity for wood that has not defibrillated. As a result, salt damage is unlikely to be the sole cause of a structural failure as engineering design requires large factors of safety.

One interesting observation in these experiments was that there was no salt efflorescence on the top surface of the sample. When this apparatus was used to measure the salt damage on stone and masonry materials, salt damage occurred both on the top of the sample and the sides of the sample (Scherer 2004). However, in these experiments, salt damage and crystallization were localized to the region immediately above the waterline.

It is likely that these patterns of salt damage are related to the porous nature of these materials. IUPAC (citation) defines three pore systems: macropores (radius greater than 50 μm), mesopores (radius between 2 and 50 μm), and micropores whose radii are less than 2 μm (Rouquerol et al 1994). Commercial softwoods are primarily a mesoporous material comprising mainly tracheids—long, narrow, empty tube-like cells whose diameter is between 5 and 40 μm and whose lumen volumes range from nearly the entire cell width in the earlywood to several micrometers in the latewood (Panshin and de Zeeuw 1980; Zillig 2009). Whether micropores exist in the cell wall is highly contested (Hill and Papadopoulos 2001). Given that wood primarily consists of large mesopores, it may not be surprising that the salt solution did not travel to the top of the wood specimens because the height of the capillary rise is inversely proportional to the radius of the pore system.

Not only does the tracheid pore system affect the capillary rise in this experiment but it also affects the proclivity of wood to exhibit damaged caused by salt. Flatt has shown that in materials with a bimodal pore size distribution, salt will tend to crystalize in the larger pore systems (Flatt 2002). In these systems, the salt crystallization will cause less damage to the material as these larger pores can accommodate the crystal and will not cause cracking or other disruption of the sound material. Because wood contains such a large volume of mesopores, wood may be, therefore, less susceptible to salt damage than other porous building materials. Furthermore, the large network of cell lumina may explain why although salt damage causes cosmetic damage to wood (Fig 1), it only causes small changes to the mechanical integrity of the wood.

Although the results from these controlled experiments give more insight into the extent of the mechanical property degradation caused by salt damage, more research is needed to understand the mechanism of salt damage in wood. Other researchers have shown that the middle lamellae of the cell walls are preferentially degraded by salt damage (Ortiz et al 2014). This suggests that salt must migrate through the cell wall from the cell lumen in part of the salt damage mechanism, and therefore, that intracell wall diffusion must play an important role in salt damage. Intracell wall diffusion is an active area of research as it is involved in many other wood decay mechanisms, such as fungal decay and fastener corrosion (Jakes et al 2013; Plaza et al 2016; Zelinka 2018; Jakes 2019). Although it is clear that salt damage must involve the diffusion of the salt to the middle lamella, the actual mechanism by which salt

weakens this structure is unclear. It could be that micropores are formed when the middle lamella is fully hydrated, which results in high crystallization pressures and cracking when the crystal nucleates. However, it is also possible that the salt chemically modifies or attacks the middle lamella. In either mechanism, developing a treatment or modification that inhibits diffusion through the cell wall should prevent salt damage in wood.

CONCLUSIONS

A method for producing salt-damaged wood under controlled laboratory conditions was presented. From the results of tests at 4 and 12 wk, the following conclusions can be drawn:

The salt water migrated less than 150 mm vertically from the surface of the water, much less than that observed for similar tests on stone and masonry materials under similar experimental conditions. Salt damage was confined to the lower half of the specimen. This was attributed to the mesoporous nature of the cell lumina.

Salt damage caused only small changes in the mechanical properties of wood as examined by the RIM. In the worst case, a 6.5% reduction in RIM was observed. It appears that a 10% reduction in structural integrity may be an upper bound on the extent of salt damage for wood that appears otherwise intact.

The mechanism for salt damage in wood must include intracell wall diffusion as one of the steps for reaction. As liquid water transport is primarily through lumina, crystallization in the lumina will not cause damage.

The current work could not differentiate whether salt damage in wood is caused by a chemical attack of the middle lamella, a nucleation of salt crystals in the same anatomical feature, or for both reasons. However, the method presented herein could be used to produce salt-damaged wood for future experiments that target differentiating these mechanisms.

REFERENCES

Anon (1992) ISO 5223 Test sieves for cereals. International Organization for Standardization, Geneva, Switzerland. 4 pp.

Brischke C, Welzbacher CR, Rapp AO (2006) Detection of fungal decay by high-energy multiple impact (HEMI) testing. Holzforschung 60(2):217-222.

Charola AE (2000) Salts in the deterioration of porous materials: An overview. J Am Inst Conserv 39(3):327-343.

Derluyn H, Dewanckele J, Boone MN, Cnudde V, Derome D, Carmeliet J (2014a) Crystallization of hydrated and anhydrous salts in porous limestone resolved by synchrotron X-ray microtomography. Nucl Instrum Methods Phys Res B 324:102-112.

Derluyn H, Moonen P, Carmeliet J (2014b) Deformation and damage due to drying-induced salt crystallization in porous limestone. J Mech Phys Solids 63:242-255.

Despot R, Hasan M, Brischke C, Welzbacher CR, Rapp AO (2007) Changes in physical, mechanical and chemical properties of wood during sterilisation by gamma radiation. Holzforschung 61(3):267-271.

Flatt RJ (2002) Salt damage in porous materials: How high supersaturations are generated. J Cryst Growth 242(3):435-454.

Glass SV, Zelinka SL (2010) Moisture relations and physical properties of wood. Pages *in* RJ Ross, ed. Wood handbook. Wood as an engineering material. U.S. Department of Agriculture, Forest Service, Forest Products Laboratory.

Greenspan L (1977) Humidity fixed points of binary saturated aqueous solutions. J Res Natl Bur Stand - A Phys Chem 81A(1):89-96.

Hill C, Papadopoulos A (2001) A review of methods used to determine the size of the cell wall microvoids of wood. J Inst Wood Sci 15(6; ISSU 90):337-345.

Jakes JE (2019) Mechanism for diffusion through secondary cell walls in lignocellulosic biomass. J Phys Chem B 123(19):4333-4339.

Jakes JE, Plaza N, Stone DS, Hunt CG, Glass SV, Zelinka SL (2013) Mechanism of transport through wood cell wall polymers. J For Prod Ind 2(6):10-13.

Johnson BR, Ibach RE, Baker AJ (1992) Effect of salt water evaporation on tracheid separation from wood surfaces. For Prod J 42(7/8):57-59.

Jones PD, Shmulsky R, Kitchens S, Barnes HM (2011) What is salt killed wood? Mississippi Cooperative Extension Service Publication 2992. Mississippi State University, Starkville, MS.

Kirker GT, Glaeser J, Lebow ST, Green F III, Clausen CA (2011) Physical deterioration of preservative treated poles and pilings exposed to salt water. Gen. Tech. Rep. FPL-GTR-203. U.S. Department of Agriculture, Forest Service, Forest Products Laboratory, Madison, WI. 7 pp.

Kirker GT, Zelinka SL, Passarini L (2016) Avast ye salty dogs: Salt damage in the context of coastal residential construction and historical maritime timbers. Pages 179-185 *in* Proc. 112th Annual Meeting of the American Wood Protection Association American Wood Protection Association, San Juan, PR.

Lewin SZ (1982) The mechanism of masonry decay through crystallization. Pages 120-144 *in* Conference on the Conservation of Historic Stone Buildings and Monuments, Washington, DC.

Ortiz R, Navarrete H, Navarrete J, Párraga M, Carrasco I, de la Vega E, Ortiz M, Herrera P, Blanchette RA (2014) Deterioration, decay and identification of fungi isolated from wooden structures at the Humberstone and Santa Laura saltpeter works: A world heritage site in Chile. Int Biodeterior Biodegrad 86:309-316.

Panshin AJ, de Zeeuw C (1980) Textbook of wood technology. Volume I. Structure, identification, uses, and properties of the commercial woods of the United States and Canada. McGraw-Hill College. 722 pp.

Parameswaran N (1981) Micromorphology of spruce timber after long-term service in a potash store house. Holz Roh Werkst 39(4):149-156.

Plaza NZ, Pingali SV, Qian S, Heller WT, Jakes JE (2016) Informing the improvement of forest products durability using small angle neutron scattering. Cellulose 23(3):1593-1607.

Price C, Brimblecombe P (1994) Preventing salt damage in porous materials. Stud Conserv 39(Supplement-2):90-93.

Rapp AO, Brischke C, Welzbacher CR (2006) Interrelationship between the severity of heat treatments and sieve fractions after impact ball milling: A mechanical test for quality control of thermally modified wood. Holzforschung 60(1):64.

Rouquerol J, Avnir D, Fairbridge C, Everett D, Haynes J, Pernicone N, Ramsay J, Sing K, Unger K (1994) Recommendations for the characterization of porous solids (Technical Report). Pure Appl Chem 66(8):1739-1758.

Scherer GW (2004) Stress from crystallization of salt. Cement Concr Res 34(9):1613-1624.

Terashima N, Fukushima K, He L-F, Takabe K (1993) Comprehensive model of the lignified plant cell wall. Pages 247-270 *in* HG Jung, DR Buxton, RD Hatfield, and J Ralph, eds. Forage and cell wall structure and digestibility. American Society of Agronomy, Madison, WI.

Zelinka SL (2018) Role of transport in wood damage mechanisms - WSE 2017 keynote lecture. Int Wood Prod J 9(2):50-57.

Zelinka SL, Kirker GT (2018) Assesment of fastener corrosion and salt damage in the bilge of the Eureka. Forest Products Laboratory Research Note FPL-RN-0356. U.S. Department of Agriculture, Forest Service, Forest Products Laboratory, Madison, WI. 12 pp.

Zillig W (2009) Moisture transport in wood using a multiscale approach. PhD dissertation, Katholieke Universiteit Leuven, Leuven, Belgium. 202 pp.

Zillig W, Janssen H, Carmeliet J, Derome D (2006) Liquid water transport in wood: Towards a mesoscopic approach. Pages 107-114 *in* Ge, Rao, and Desmarais, eds. Research in building physics and building engineering. Taylor and Francis Group, London.